COPY RIGHT

Title:- High Speed Sensor Networks For Air Quality Monitoring Applications.

Paper Authors

N SUMALATHA, P SRILAXMI, P GOWTHAMI

Dept of ECE, SV University.

USE THIS BARCODE TO ACCESS YOUR ONLINE PAPER

To Secure Your Paper As Per UGC Approvals We Are Providing A Electronic Bar Code

HIGH SPEED SENSOR NETWORKS FOR AIR QUALITY MONITORING APPLICATIONS

[1]N SUMALATHA, [2]P SRILAXMI, [3]P GOWTHAMI

[123] Dept of ECE, SV University, Tirupati, AP, India.

nalukurthisumalatha@gmail   kalikanda@gmail.com   gowthami0055@gmail.com.

ABSTRACT— This paper gives a community for indoor and out- door air pleasant tracking. Each node is hooked up in a specific room and consists of tin dioxide sensor arrays related to an acquisition and manage device. The nodes are hardwired or twine-lessly linked to a significant tracking unit. To boom the fuel concentration dimension accuracy and to prevent false alarms, gas sensor have an impact on portions, i.E., temperature and humidity, also are measured. Advanced processing based on more than one-enter– single-output neural networks is applied at the community sensing nodes to achieve temperature and humidity compensated gasoline attention values. Anomalous operation of the network sensing nodes and strength intake are also discussed.

Key Terms—Air quality (AirQ), embedded Web server, neural network, wireless networks.

I.INTRODUCTION

AIR supplies us with oxygen that is essential for our bodies to live. Air is 99.9% nitrogen, oxygen, water vapor, andinert gases. Human activities can release substances into the air, some of which can cause problems for humans, plants, and animals. Air quality can be expressed by the concentration of several pollutants such as carbon monoxide (CO), sulphur dioxide, nitrogen dioxide, and ozone. The threshold values specified by the European Environment Agency [1] for these pollutants are 10, 350, 40, and 120 µg/m3, respectively. Pollution also needs to be considered inside our homes, offices, and schools. Some of these pollutants can be created by indoor activities such as smoking and cooking. Generally, in industrialized countries, the population spends about 80%–90% of time inside buildings and is therefore exposed to harmful indoor pollutants. Indoor air quality is generally assessed by separately measuring CO, temperature, and humidity [2]. This information, even if fused, is insufficient to allow a good characterization of indoor air quality. The development of wireless local area network (WLAN; IEEE802.11X) technology and the marketing of low-cost access points (APs; e.g., Linksys WAP11), wireless network adapters (CardBus; e.g., D-Link DWL-G650+), and wireless bridges (e.g., DWL-810+) creates the possibility of implementing indoor/outdoor air quality monitoring networks characterized by high flexibility, modularity, and low cost. Tin oxide sensors (e.g., Figaro, Nemoto [3]) are inexpensive and fair selective gas sensors. To overcome some of their limitations such as cross sensitivities [4], [5] and a temperature and humidity dependence behavior [6], appropriate sensor data processing is required. The aim of this work is to present a Wi-Fi indoor—outdoor air quality monitoring network that combines the capabilities of tin

oxide sensors with advanced sensor data processing based on multilayer perceptron neural networks for an accurate measurement of air quality and for the detection of air pollution events and of sensors' abnormal operation.

II. DIRECT AND INVERSE MODELING OF THE SENSORS' CHARACTERISTICS

The sensors' nonlinearity requires the utilization of direct and inverse modeling for sensor calibration and on-line measurement phase [7]. For the particular case of tin oxide gas sensors TGS800, TGS822, TGS842, and TGS203, the sensors' response is strongly dependent on parameters such as temperature, humidity, and cross influence of the other gases. For practical and economic reasons, the number of calibration points is very low, and thus, a neural network (multilayer perceptron architecture), which is a global approximator of multivariable characteristics [8], was used in this paper. Polynomial modeling is another solution for multivariable characteristics modeling. Representative of this type of solution is the polynomial model that is a part of the IEEE1451.2 standard for smart sensors particularly related to smart sensors correction engine implementation[9]. The method represents an interesting solution.

However, it requires a large set of data (i.e., a higher number of calibration points compared with a neuronal network model) for polynomial model coefficients calculation [10], i.e.,

$$\sum_{i=0}^{D(1)} \sum_{j=0}^{D(2)} \cdots \sum_{p=0}^{D(n)} C_{i,j,\ldots,p} [X_1 - H_1]^j [X_2 - H_2]^j \cdots [X_n - H_n]^p \quad (1)$$

where Xn are the input variables to the sensor characteristic block, Hn are the offsets to the input variables, and the $D(k)$ represents the degree of the input Xk, i.e., the highest power to which $[Xk - Hk]$ is raised in any term of the multinomial. The $Ci,j,\ldots,p$ represent the calculated correction coefficients for each term values that are obtained, considering the segmentation of the input variable range. The accuracy of the method is influenced by the polynomial degree, the number of segments, and the number of values included in defined subranges that make the multivariable polynomial inverse modeling for external factors compensation computationally expensive. Considering only one segment for a given gas concentration, where the voltage acquired from gas sensor channel represents the primary variable ($X1 = VGi$), and restricting the number of influence factors on gas concentration measurement to temperature and humidity expressed by voltage values acquired from temperature and relative humidity sensor channels ($X2 = VT, X3 = VRH$), the compensated values of gas concentration CGi are expressed by

$CGi = C000 + C100CGi + C010VT + C001VRH + C101VGiVRH + C110VGiVT + C011VT\ VRH + C111VGiVT\ VRH.$ (2)

As can be observed, to reduce the complexity the first-degree polynomial approximation is considered. Better accuracy can be obtained with a higher degree multivariable polynomial model, which implies an increase of the computational load. A comparison between the "classical" polynomial modeling and neural network modeling shows that the number of calibration points used to calculate the polynomial coefficients for an imposed

accuracy of inverse characteristic modeling is generally greater than the number of calibration points used to design the neuronal network sensor models [11]. Moving the complex processing from the embedded server to the Web browser side permits us to overcome some of the drawbacks of neural network processing such as the high number of multiplication and the use of nonlinear transfer functions (e.g., $\tanh(\cdot)$).

III. SENSORS' NETWORK

Gas sensor networks provide a promising mechanism for mining information from the monitored areas. The following two types of Wi-Fi (WLAN) architectures were considered: 1) an ad hoc architecture and 2) an AP infrastructure network, which assures additional services (e.g., data publishing on the wired Internet), taking into account that the AP works like a bridge between the wired and wireless network [12]. The ad hoc architecture seems to be a good solution, particularly for air quality monitoring in outdoor conditions since it requires less elements and, thus, less power consumption.

The ad hoc smart sensor network (Fig. 1, case 1) includes the following three elements: 1) a PC with an IEEE802.11gcompatible Wi-Fi cardbus adapter (DWL-G650+) as the main control and processing unit; 2) a set of sensing nodes (SNj) with air quality sensors (GS1, GS2, . . . , GSi); and 3) a data acquisition, primary processing, and transmission control protocol/Internet protocol (TCP/IP) communication unit (APC) based on IPμ8930 general-purpose network controller whose Ethernet port is connected to a DWL-G810 wireless bridge.

Referring to the AP infrastructure (case 2), the wireless network node components are the same as that of case 1, with the only difference being the inclusion of an AP (LinksysWAP11), which is an element that extends the wireless subnetwork
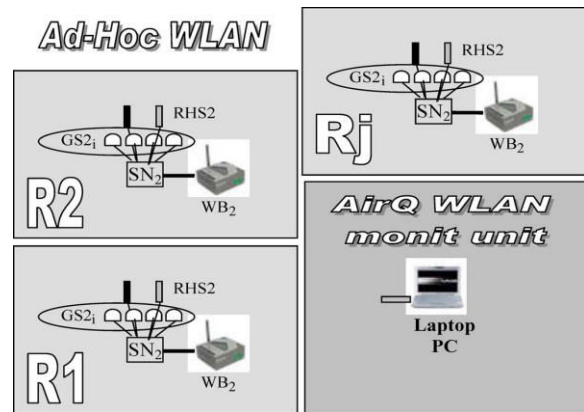
Fig. 1. Ad hoc air quality smart sensor network architecture associated with different rooms (R1, R2, . . ., Rj), where SNj are sensing nodes, GSj i are gas sensors, TSj are temperature sensors, RHSj are relative humidity sensors, and WBj are wireless bridges.
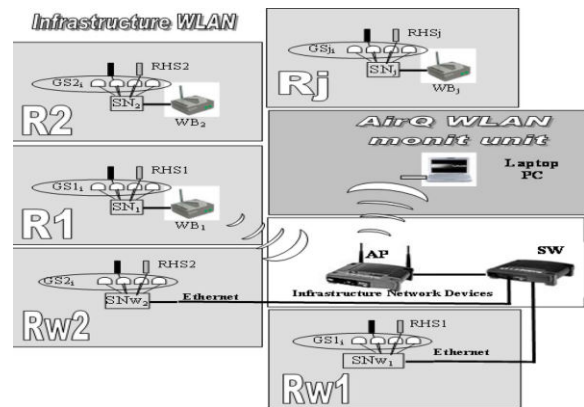
Fig. 2. Infrastructure WLAN air quality smart sensor network architecture that includes sensing nodes distributed in different rooms. R1, . . ., Rj: Rooms with wireless sensing

nodes. Rw1 and Rw2: Rooms with wired sensing nodes. SNj : Sensing nodes. GSj i: Gas sensors. TSj : Temperature sensors. RHSj : Relative humidity sensors. WBj : Wireless bridges. AP: Access point.

range capabilities and enables wireless network traffic to be transmitted over the wired network that can include additional wired sensing nodes (SNj) distributed in different rooms (Rwj rooms; Fig. 2). As can be observed in Fig. 2, the wireless or wired sensing nodes are installed in different rooms (R1, R2, . . . ,Rj, Rw1, Rw2, . . . ,Rwj), where different values of temperature, relative humidity, and air quality are measured. Fig. 3 underlines the differences between the measured air quality parameters in the
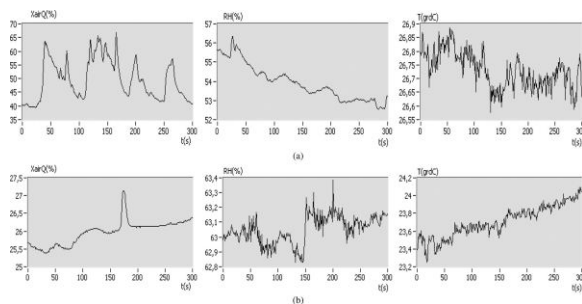
Fig. 3. Time evolution of indoor air quality parameters in two different rooms. (a) Smoking room. (b) Non-smoking room.

following two different situations: 1) smoking room and 2) nonsmoking room.

A. Sensing Nodes

The sensing nodes are designed and implemented to perform the air quality ($AirQ$) monitoring using low-cost gas sensors and, at the same time, to get the additional information about the temperature T and relative humidity RH. This information is used to increase gas concentration measurement accuracy performing the error compensation caused by temperature and humidity influence.

The used gas sensors are sintered using SnO2 semiconductor heated sensors provided by Figaro [13] that assure pollution event detection (TGS800-general air contaminant sensor-AC), methane detection (TGS842-M), alcohol and organic solvent detection (TGS822-SV), and CO detection (TGS203-CO). Information about temperature and relative humidity are obtained using Smartec SMT160-30 [14] and Humirel HM1500 [15] temperature and relative humidity transducers, respectively.

The sensor experimental direct characteristics are expressed by voltages obtained at the gas sensor conditioning circuit output for different concentrations of gas, expressed in parts per million. The used conditioning circuit for the air pollution sensor TGS800, solvent vapors (TGS822), and methane sensor (TGS842) are presented in Fig. 4.

To perform the sensor characterization, each of the considered gas sensors (GSi) is separately introduced in a test chamber as part of a laboratory-developed gas sensor calibration system. The values of gas concentration are imposed using a mass flow controller (MC Alicat Scientific) connected to gas bottles with standard concentration (e.g., 100 ppm CO). Temperature and humidity are measured using the temperature and relative humidity sensors that are also included in the chamber. Different values of temperature and relative humidity
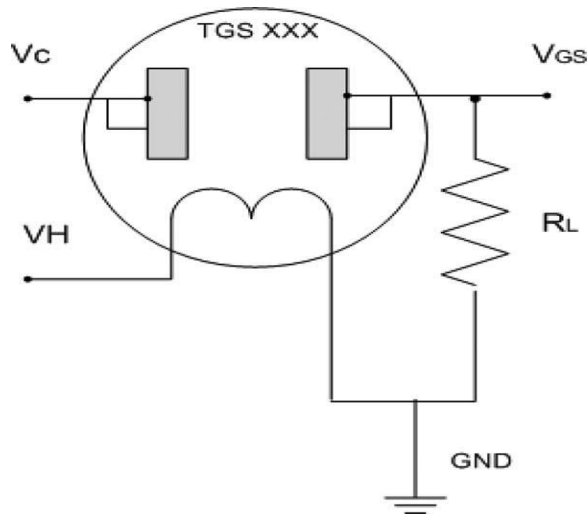
Fig. 4. Gas sensor conditioning circuit. *Vc*: Circuit voltage. *VH*: Heater voltage. *VGS*: Gas sensor output voltage. *R*L: Load resistance.

are imposed employing a set of drying and saturation chambers connected to the testing chamber and air pumps (Fig. 5). To decrease humidity, the drying chamber with two Peltier cells is connected to the test chamber.

After condensation on the Peltier cells surface, the condensed liquid in the drying chamber is collected and pumped off from the drying chamber. Low values of relative humidity can be obtained in this way (e.g., *RH* = 20%). Higher humidity values are obtained when the saturation chamber is connected to the testing chamber. In this case, condensed/distilled water is pumped from the water tank and vaporized into the air circulation system. Values of 95% were reached using this procedure. Using the *RH* variation procedure, gas sensors characteristics for *RH*1 = 35%, *RH*2 =65% and *RH*3 = 95% were obtained.

For temperature, a Peltier cell is employed. Additionally, a testing chamber ventilator is used to inject the cold or warm the air in the testing chamber. For the considered case, several
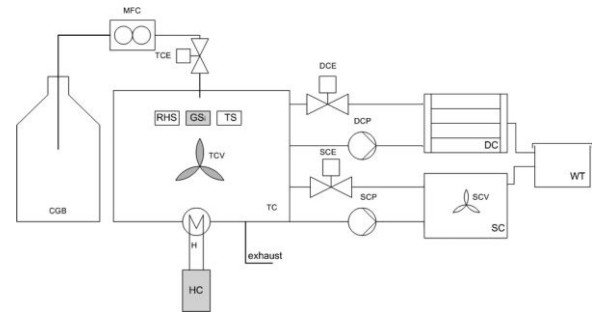
Fig. 5. Gas sensor calibration system architecture. CGB: Calibration gas bottle. MFC: Mass flow control. TCE: Testing chamber electrovalve. DCE: Drying chamber electrovalve. SC: Saturation chamber electrovalve. DCP: Drying chamber pump. SCP: Saturation chamber pump. DC: Drying chamber. SC: Saturation chamber. HC: Heater control. H: Heater. WT: Water tank. TCV: Testing chamber ventilator. SCV: Saturation chamber ventilator.

values of temperature were imposed, *T*1 = 10 ◦C, *T*2 = 15 ◦C; *T*3 = 20 ◦C, *T*4 = 25 ◦C and *T*5 = 30 ◦C.

A gas exhaust circuit is used to clean the testing chamber after a particular gas sensor testing (e.g., TGS842 Methane gas sensor testing).

B. APC

The voltages obtained from sensors' channels are applied to the analog inputs of the APC, which is a general-purpose network controller and Web server (Ipsil IPμ8930). It performs sensing channels data conversion (voltage to gas concentration in parts per million, voltage to temperature in degrees Celsius, and voltage to relative humidity in percent) and Web

data publishing (case 1) or transmits the data using TCP/IP communication to the main processing and control unit (laptop PC) that performs the data logging, data processing, and

Webpublishing through a LabVIEW Web server (case 2).

IV. DATA PROCESSING

Two types of sensor data processing architectures that allow the calculation of several air quality values are implemented using JavaScript and LabVIEW Web publisher technologies.

The first one is a neural network algorithm implemented in JavaScript in the embedded server (Web sensor) and represents one of the main novelties of the work. The second software architecture is implemented in the network PC and performs the following three tasks: 1) sensing nodes data reading through TCP/IP remote control; 2) air pollution events detection and gas concentration estimation based on neural network inverse models of gas sensors; and 3) data logging and Web publishing of air quality data. The LabVIEW capabilities were used for the implementation of this architecture. JavaScript is associated to the smart sensor network and assures independent dynamic webpages generation. The sensor nodes (SNj), which are supported by embedded Web server architectures, acquire and process the voltages from sensors' channels using a set of implemented JavaScript functions (JSi) that are part of hypertext markup language (HTML) files stored in an embedded Web server (Ipsil IPμ8930) electrically erasable programmable read-only memory (EEPROM). JSi complexity depends on the associated sensor. Data processing is performed mainly at the Web browser level, which reduces the computational load associated with embedded Web servers and is also important as regard power consumption and Web server autonomy.

Referring to the JST and JSRH, which are JavaScript functions associated with temperature and relative humidity calculation, the following relations are implemented:

$$T = \alpha_1 \times \left(\frac{V_T}{V_S} - \beta_1 \right) \quad RH = \alpha_2 \times \left(\frac{V_{RH}}{V_S} - \beta_2 \right) \quad (3)$$

where α_1 = 212.765 °C, β_1 = 0.320, α_2 = 210.970 % RH, β_2 = 0.235, V_S = +5 V, V_T is the temperature channel's voltage, and V_{RH} is the relative humidity channel's voltage. In the GSi case, a set of JSNPBi (JavaScript neural processing block for i measurement channel: NPBi) functions are used.

The utilization of NPBs is related with the inverse modeling [16] of gas sensor multivariable nonlinear characteristics, which are strongly dependent on temperature and humidity but are also influenced by the concentration of other gases as part of the analyzed gas mixture. Based on the designed NPBi, a

digital readout of the gas concentration with temperature and compensation [17] is obtained.

A. NPBi Architecture and Design

The used neural processing blocks (NPBi) are two inputs-one output multilayer perceptron neural networks (Fig. 6).
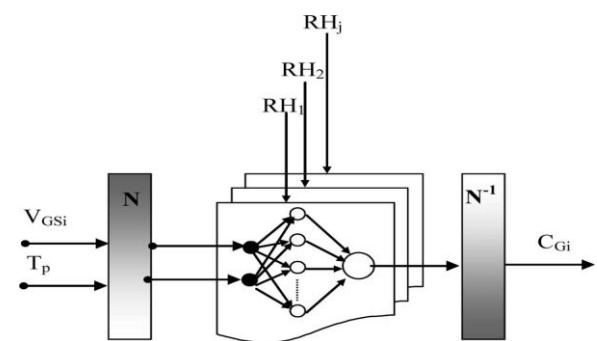
Fig. 6. The NPBi architecture. N, $N-1$: Normalization and denormalization blocks. RHj : Humidity selector. CGi : Temperature and

humidity compensated values of the gas concentration Gi. TP : Temperature input value. $VGSi$: Input voltage value on the GSi channel.

The NPBi's internal parameters (weights and biases) are calculated offline using MATLAB. The neural network training data were obtained in the system calibration phase. They are voltage values ($VGSi$) acquired from the gas concentration measurement channel for different values of gas concentration CGi and different temperature (Tp) and relative humidity (RHi) conditions.

The developed MATLAB neural network design program calculates different sets of weights and biases for each RHi experimental value (e.g., $RH = \{45\%, 55\%, 65\%\}$. In the air quality parameters measuring phase, the calculated weights are used by JavaScript- or LabVIEW-implemented functions for online processing of the acquired voltages.

The NPBi inputs are the normalized voltages associated with gas sensors' channels and a normalized temperature, while the NPBi's output is the temperature-compensated gas concentration CGi. The NPBi normalized inputs are defined by

$$V_{GS_i}^N = \frac{V_{GS_i}}{V1_s} \quad T^N = \frac{T}{\max(T)} \quad (4)$$

where $V 1S$ represents the gas sensor normalization factor (GSi voltage supply = +10 V in this paper).

Because GSi characteristics depend on humidity [13], an accurate measurement of the gas concentration is provided using different NPBi|RHs whose weights and biases are calculated using data obtained for different relative humidity conditions (i.e., $RH = 45\%$, 55%, and 65%) and the interpolation method

presented in [18].

The number of NPBi's layers is three. The hidden layers have two to five tansignoid ($\text{tansig}(x)$) neurons, and the output layer has one linear ($l(x)$) neuron. The implemented $\text{tansig}(x)$ calculate its output according to

$$\text{tansig}(x) = \frac{2}{1 + \exp(-2x)} - 1 \qquad (5)$$

which leads to a reduction in the computational load.

Two criteria for NPBi design were considered, namely, the type and the number of neurons on the hidden layer, both determining the capabilities of the NPBi to adapt to a given
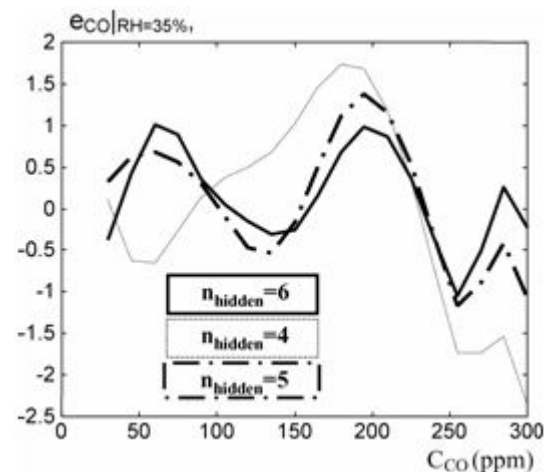
Fig. 7. Modeling error versus concentration for different NPBCO architectures ($T = 10$ °C).

characteristic. Different neuron nonlinear activation functions require different memory space and processing capabilities from the hardware platform. In this paper (tansignoid activation function), the neural processing task is distributed between the sensing node, which includes an embedded Web server, and the Web client (laptop PC), thus reducing the requirements of complex processing at the IPμ8930 level. At the same time, and considering the IPμ8930 memory space, an

optimization of HTML number of pages and the page size was carried out.

To diminish the vector sizes of weights and biases, a study concerning the number of neurons for a required NPBi performance, which is expressed by a modeling error, was also carried out. More neurons imply complex processing but, first, imply large dimensions of the weights and biases matrices, which mean large memory requirements. Thus, the objective was to reduce the number of hidden neurons, taking into account the limited memory resources (512 kB EEPROM) of the IPμ8930 and the browser's online sensor data processing capabilities.

For the particular case of the CO measuring channel, the training set includes, as target, 15 CO concentration values uniformly distributed in the 30–300 ppm interval. The input values are the voltage values acquired from the TGS203 CO concentration measuring channel corresponding to the aforementioned concentrations. The measured temperature in the testing chamber was Tp [in degrees Celsius] = $10 \times p$, $p = \{1, 2, 3, 4, 5\}$, and the relative humidity was $RH = 35\%$. The Levenberg–Marquardt algorithm [19] was used to calculate the weights and biases (i.e., WNPBi and BNPBi) of the neural network. Imposing a sum square error stop condition SSE = 0.01, and for neural networks characterized by four, five, or and hidden neurons, different measuring channel modeling error characteristics (eCGsi) were obtained (Fig. 7). The modeling error is defined by

$$e_{\text{CGsi}} = \frac{C_{\text{CGsi}} - C_{\text{CGsi}}^{\text{NPB}}}{\text{FS}} \times 100 \qquad (6)$$

where FS represents the measurement range, CCGsi is the experimental used gas

concentration (e.g., CO concentration) expressed in parts per million, and CNPB CGsi is the concentration of gas calculated by the corresponding neural processing module.
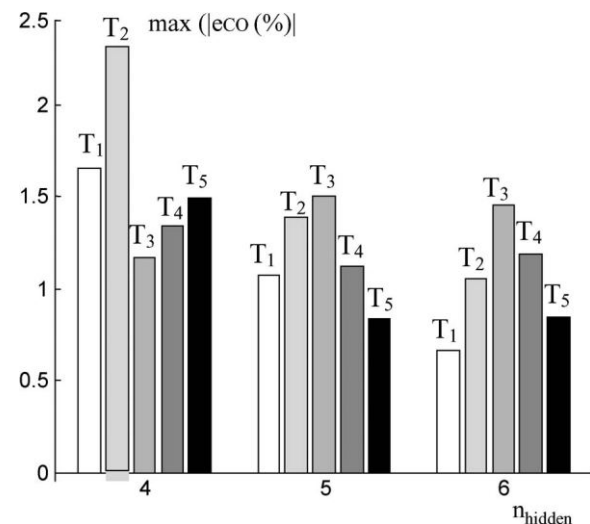
Fig. 8. Maximum inverse modeling error for different NPBCO architectures ($n$hidden = {4, 5, 6}) and different temperatures $Tp = 10p$ °C.

Since the used gas sensors characteristic depends on temperature, a study related with the CO channel modeling error (eCO) versus temperature was carried out (Fig. 8). With humidity being an influence quantity, different values of the relative humidity lead to different primary gas selectivity characteristics and, hence, to different gas concentration measurement accuracies. Thus, experimental data obtained for three different values of relative humidity, i.e., $RH1 = 35\%$, $RH2 = 65\%$, and $RH3 = 95\%$, and five values of temperatures included in the $IT = [10; 50]$°C were considered. The

imposed gas concentrations for measurement system testing were ten values of methane concentration distributed in the ICM = [500; 5000] ppm interval, 15 values of CO concentration ICCO = [30; 300] ppm, and 15

values of solvent vapors (ethanol vapors) concentration, i.e., $CSV = [50; 5000]$ ppm.

Based on the GSi voltages for the considered gases concentrations, and taking into account temperature and humidity, three sets of weights and biases (35%, 65%, and 95% relative humidity) were calculated for CO, methane, and solvent vapor measurement channel.

VII. CONCLUSION

This paper has reported the implementation of a measuring system for air quality monitoring. Two architectures are proposed for wireless communication between the sensing nodes and a personal computer that manages the whole system. Because of the communication range of the hardware used, the systems are particularly suited for indoor applications. The outdoor range limitation can be overcome using high-gain omnidirectional antennas (e.g., D-Link ANT24-1500) that provide extended coverage for an existing 802.11b/g wireless network avoiding the cost and complexity of adding additional wireless APs or wireless repeaters. The coverage of the Wi-Fi designed network can be extended up to tens of kilometers by including in the system extended coverage Wi-Fi repeaters (e.g., Duganit WL-2410).

Considering the increasing number of the low-cost or even free Wi-Fi Internet hotspots and the capabilities of the distributed air-quality-developed system (based on air-qualityembedded Web sensors), different locations can be monitored and the air quality values Web published as long as they have Wi-Fi coverage. The output of the used gas sensors depends not only on the cross influence of the primary measured gas but also on external influence factors, namely temperature and humidity. Thus, several NPBs were implemented to obtain the temperature and humidity corrected values of the gases' concentrations. The merits of this type of technique for the required purpose, i.e., the accurate inverse modeling of the gas measuring channel for a small number of calibration points, are well established.

The main novelties of this paper are given as follows:

1) the development of an air quality monitoring system that uses smart sensors in a wireless network; 2) the embedding of neural network processing blocks distributing the processing charge between the embedded systems (Web sensor) and the Web browser installed in a personal computer; and 3) the development of PC software for sensing node TCP/IP remote control, advanced data processing, data storage, and Web publishing software associated with air quality monitoring system. Special attention was granted to the optimal implementation of the neural network and to a practical evaluation of the distributed sensing system power consumption.

The proposed air quality monitoring system based on a wireless smart sensor network and on neural network processing blocks embedded on the sensing nodes' HTML pages presents the following advantages.

• It provides extended capabilities for air quality monitoring for indoor and outdoor conditions.

• It provides good accuracy of gas concentration measurements by using neural networks to compensate the temperature and humidity influences.

• It presents a client-side JavaScript solution for neural network implementation.

• Based on TCP/IP read and write functions implemented in LabVIEW, it allows advanced processing of air quality data by a PC.

Measurements of the system's power requirements show that each node requires about 8 W. This clearly indicates that a system's autonomy of days or months can only be reached if batteries' recharge capability, using, for instance, solar panels, is provided.

The output of a specific tin dioxide sensor arrays depends not only on temperature and humidity but also on the concentration of other gases and vapors. The effect of this cross influence on the accuracy of the measurement can be minimized using also neural networks.We will address this problem in a future work.

REFERENCES

[1] European Environment Agency, *Air Pollution*, 2001. Report.

[2] J. Bartolomeo, "Detecting CO in the home," *Home Automation and Building Control*, pp. 51–55, Oct. 1995.

[3] *Nemoto Chemical Sensors Catalogue*, Nemoto & Co., Tokyo, Japan. [Online]. Available: http://www.nemoto.co.jp/product

[4] F. Sarry and M. Lumbreras, "Gas discrimination in an air-conditioned system," *IEEE Trans. Instrum. Meas.*, vol. 49, no. 4, pp. 809–812, Aug. 2000.

[5] S. Marco, A. Ortega, A. Pardo, and J. Samitier, "Gas identification with tin oxide sensor array and self-organizing maps: Adaptive correction of sensor drifts," *IEEE Trans. Instrum. Meas.*, vol. 47, no. 1, pp. 316–320, Feb. 1998.

[6] A. Lee and B. Reedy, "Temperature modulation in semiconductor gas sensing," *Sens. Actuators B, Chem.*, vol. 60, no. 1, pp. 35–42, Nov. 2, 1999.

[7] F. Ménil, M. Susbielles, H. Debéda, C. Lucat, and P. Tardy, "Evidence of a correlation between the non-linearity of chemical sensors and the asymmetry of their response and recovery curves," *Sens. Actuators B, Chem.*, vol. 106, no. 1, pp. 407–423, Apr. 29, 2005.

[8] R. Selmic and F. L. Lewis, "Neural-network approximation of piecewise continuous functions: Application to friction compensation," *IEEE Trans. Neural Netw.*, vol. 13, no. 3, pp. 745–751, May 2002.

[9] H. G. Ramos, J. M. Dias Pereira, V. Viegas, O. Postolache, and
P. M. B. Silva Girão, "A virtual instrument to test smart transducer interface modules (STIMs)," *IEEE Trans. Instrum. Meas.*, vol. 53, no. 4, pp. 1232–1239, Aug. 2004.